Mito-FUNCAT-FACS reveals cellular heterogeneity in mitochondrial translation

YUSUKE KIMURA,[1,2,5] HIRONORI SAITO,[1,2,5] TATSUYA OSAKI,[3] YASUHIRO IKEGAMI,[3] TAISEI WAKIGAWA,[1,2] YOSHIHO IKEUCHI,[3,4] and SHINTARO IWASAKI[1,2]

[1]Department of Computational Biology and Medical Sciences, Graduate School of Frontier Sciences, The University of Tokyo, Kashiwa, Chiba 277-8561, Japan

[2]RNA Systems Biochemistry Laboratory, RIKEN Cluster for Pioneering Research, Wako, Saitama 351-0198, Japan

[3]Institute of Industrial Science, The University of Tokyo, Meguro-ku, Tokyo 153-8505, Japan

[4]Institute for AI and Beyond, The University of Tokyo, Bunkyo-ku, Tokyo 113-0033, Japan

ABSTRACT

Mitochondria possess their own genome that encodes components of oxidative phosphorylation (OXPHOS) complexes, and mitochondrial ribosomes within the organelle translate the mRNAs expressed from the mitochondrial genome. Given the differential OXPHOS activity observed in diverse cell types, cell growth conditions, and other circumstances, cellular heterogeneity in mitochondrial translation can be expected. Although individual protein products translated in mitochondria have been monitored, the lack of techniques that address the variation in overall mitochondrial protein synthesis in cell populations poses analytic challenges. Here, we adapted mitochondrial-specific fluorescent noncanonical amino acid tagging (FUNCAT) for use with fluorescence-activated cell sorting (FACS) and developed mito-FUNCAT-FACS. The click chemistry-compatible methionine analog L-homopropargylglycine (HPG) enabled the metabolic labeling of newly synthesized proteins. In the presence of cytosolic translation inhibitors, HPG was selectively incorporated into mitochondrial nascent proteins and conjugated to fluorophores via the click reaction (mito-FUNCAT). The application of in situ mito-FUNCAT to flow cytometry allowed us to separate changes in net mitochondrial translation activity from those of the organelle mass and detect variations in mitochondrial translation in cancer cells. Our approach provides a useful methodology for examining mitochondrial protein synthesis in individual cells.

Keywords: FACS; FUNCAT; HPG; mitochondria; translation

INTRODUCTION

Mitochondria are the major suppliers of cellular ATP via oxidative phosphorylation (OXPHOS). As a consequence of symbiosis with a bacterial ancestor, the mitochondrion maintains its own genome and expresses its own genes. In addition to noncoding RNAs (2 rRNAs and 22 tRNAs), mammalian mitochondrial DNA (mtDNA) encodes 13 mRNAs that are essential components of OXPHOS complexes (Anderson et al. 1981). Impairment of mitochondrial translation, for example, dysfunction of mitochondrial tRNAs, often causes OXPHOS dysfunction and leads to diseases (Scharfe et al. 2009; De Silva et al. 2015; Suomalainen and Battersby 2018; Webb et al. 2020), including mitochondrial myopathy, encephalopathy, lactic acidosis, and stroke-like episodes (MELAS) and myoclonic epilepsy with ragged-red fibers (MERRF) (Yasukawa et al. 2000a,b; Kirino et al. 2005; Rötig 2011; Keilland et al. 2016; Asano et al. 2018; Morscher et al. 2018).

Mitochondrial protein synthesis is driven by 55S mitochondrial ribosomes (or mitoribosomes). Owing to the recent emergence of structures at near-atomic resolutions, the architecture of mitoribosomes has been revealed to be distinct from bacterial and eukaryotic cytoplasmic ribosomes (or cytoribosomes) (Kummer and Ban 2021). In organello translation has been investigated through various approaches, such as the following: (1) sucrose density gradient ultracentrifugation for polysome isolation and subsequent mRNA quantification via quantitative reverse transcription-PCR (RT-qPCR) or northern blotting (Antonicka et al. 2013; Fung et al. 2013; Grimes et al. 2014; Zhang et al. 2014; Pearce et al. 2017; Cahoon and Qureshi

2018); (2) ribosome profiling (Iwasaki et al. 2016; Suzuki et al. 2020; Kashiwagi et al. 2021), a method based on RNase footprinting by ribosomes and following deep sequencing (Ingolia et al. 2009), and the derivative methods tailored for mitochondrial translation (Rooijers et al. 2013; Couvillion et al. 2016; Couvillion and Churchman 2017; Gao et al. 2017; Pearce et al. 2017; Morscher et al. 2018; Li et al. 2021; Schöller et al. 2021); (3) pulsed stable isotope labeling by amino acids in cell culture (pSILAC) following mass spectrometry (Imami et al. 2021); (4) in situ cryo-electron tomography (Pfeffer et al. 2015; Englmeier et al. 2017); (5) in vitro reconstitution with purified factors (Lee et al. 2021); and (6) in vitro silencing of translation in purified mitochondria (Cruz-Zaragoza et al. 2021).

The most conventional method used by mitochondrial protein synthesis studies is to label translation products with radioactive amino acids (e.g., L-[35S]-methionine). The relatively large pool of cytoribosomes and translation products hinders the detection of proteins synthesized in mitochondria. Thus, cells are treated with cytoribosome-specific inhibitors such as cycloheximide (CHX), anisomycin (ANS), and emetine (EME) (Garreau de Loubresse et al. 2014; Wong et al. 2014) to suppress cytosolic translation, allowing specific labeling of mitoribosome-synthesizing proteins (Jeffreys and Craig 1976; Weraarpachai et al. 2009).

Despite the high sensitivity of the radioactive labeling of nascent proteins, the availability of alternative methods involving fluorescence is also an advantage (regardless of whether translation occurs in the cytoplasm or mitochondria) since these alternative methods are applicable to microscopy and flow cytometry analyses (Iwasaki and Ingolia 2017). The metabolic incorporation of methionine analogs with click-reactive moieties, such as L-homopropargylglycine (HPG) and L-azidohomoalanine (AHA) (Supplemental Fig. S1A), allows the conjugation of fluorophores to proteins synthesized during a given period. This technique, called fluorescent noncanonical amino acid tagging (FUNCAT), is used to measure cytosolic translation via sodium dodecyl sulfate-polyacrylamide gel electrophoresis (SDS-PAGE) (Yoon et al. 2012), microscopy (Beatty et al. 2006; Beatty and Tirrell 2008; Roche et al. 2009; Dieterich et al. 2010; Tcherkezian et al. 2010; Hinz et al. 2012; Yoon et al. 2012), or flow cytometry (Beatty and Tirrell 2008; Signer et al. 2014).

In contrast to cytosolic translation, the application of FUNCAT to mitochondrial translation (mito-FUNCAT) has been restricted to bulk on-gel assays (Zhang et al. 2014) (on-gel mito-FUNCAT) and microscopy analyses (Estell et al. 2017; Yousefi et al. 2021; Zorkau et al. 2021) (in situ mito-FUNCAT) (Supplemental Fig. S1B). However, these approaches (and the other methods mentioned above) may miss a subpopulation of cells, because bulk on-gel assays average all cells and microscopy covers only a limited number of cells. In this work, we developed

the mito-FUNCAT-fluorescence-activated cell sorting (FACS) method for the high-throughput quantification of mitochondrial protein synthesis in cells in response to biogenesis and functional activation of mitochondria and investigated the cellular heterogeneity of in organello translation.

RESULTS AND DISCUSSION

In-cell visualization of mitochondrial protein synthesis

To investigate mitochondrial translation, we metabolically labeled newly synthesized proteins generated within mitochondria with the click-reactive methionine analogs HPG and AHA (Supplemental Fig. S1A). Although these analogs can be incorporated into both cytosolic and mitochondrial nascent peptides, halting cytosolic translation with the cytoribosome-specific inhibitor ANS (Garreau de Loubresse et al. 2014) resulted in only active mitochondrial translation over a given period of analog incubation (Fig. 1A). The resultant HPG-labeled nascent proteins were conjugated with fluorophores via an in vitro click reaction and visualized via SDS-PAGE (on-gel mito-FUNCAT) (Fig. 1B; Supplemental Fig. S1B). Essentially, the same pattern of signals was obtained with other cytosolic translation inhibitors, CHX and EME (Supplemental Fig. S1C). The use of this method was further validated for the assessment of mitochondrial protein synthesis by the recovery of "HPGylated" proteins in the mitochondrial fraction (Fig. 1B), the disappearance of these proteins by treatment with chloramphenicol (CAP) (Fig. 1B), an inhibitor of prokaryotic/mitochondrial ribosomes (Grivell et al. 1971; Dunkle et al. 2010), and the assignment of 13 mtDNA-encoded proteins by their molecular weight (Supplemental Fig. S1D). Although AHA also enabled the detection of ANS-resistant signals, this analog provided a higher background signal (Supplemental Fig. S1E). The higher background signal may be due to nonspecific labeling induced by terminal alkynes, as suggested in an earlier study (Speers and Cravatt 2004; Ali et al. 2019). Thus, in this study, we used HPG instead of AHA for the downstream assays.

Taking advantage of the lower background of HPG in the click reaction, we applied this technique to an in-cell reaction (in situ mito-FUNCAT) (Supplemental Fig. S1B). As expected, we observed that the FUNCAT signal was overlaid with a mitochondrial marker (MitoTracker) (Fig. 1C). This approach was not only restricted to mouse C2C12 cells (Fig. 1C), as reported in earlier work (Estell et al. 2017), but also succeeded in human HEK293 and HeLa S3 cells (Fig. 1D), suggesting the versatility of in situ mito-FUNCAT in a wide array of cells (Yousefi et al. 2021; Zorkau et al. 2021). Note that we used a lower concentration of HPG (50 μM for on-gel and 100 μM for in situ
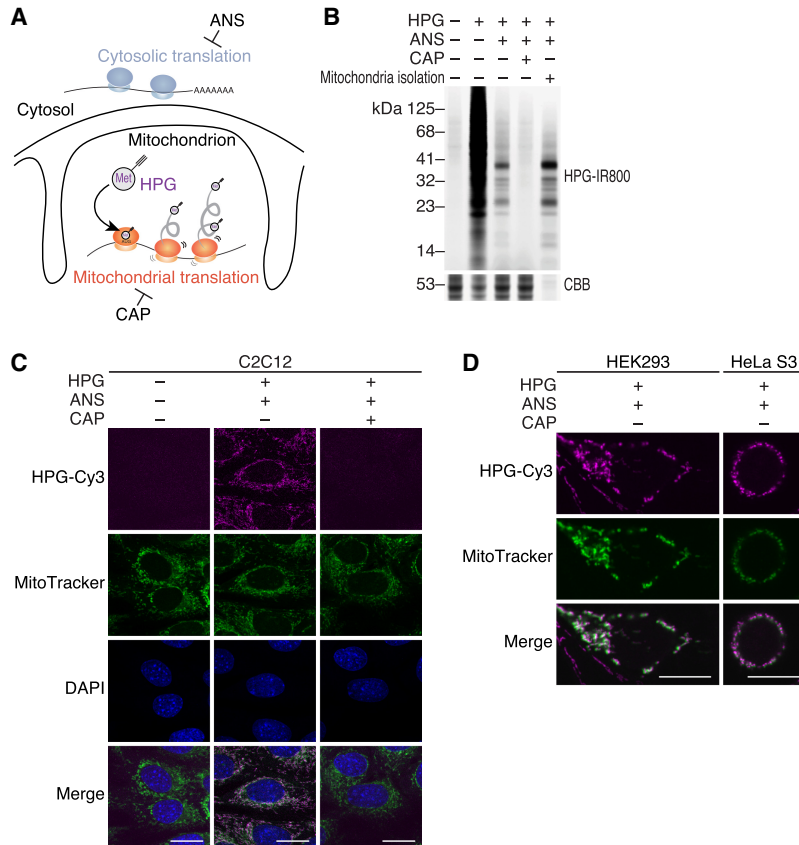
FIGURE 1. On-gel and in situ mito-FUNCAT in mammalian cell lines. (*A*) Schematic presentation of the experimental design. Mitochondrial nascent proteins were specifically labeled with a methionine analog, L-homopropargylglycine (HPG), while cytosolic translation was halted with anisomycin (ANS). As a control, mitochondrial translation was also blocked by chloramphenicol (CAP). (*B*) Representative gel images (*n* = 5) of total and mitochondrial nascent proteins. HEK293 cells were incubated with HPG in the presence or absence of inhibitors (ANS and CAP). Infrared (IR)-800 dye was conjugated to HPG-containing nascent proteins via a click reaction. Total protein was stained with CBB. (*C*) Representative micrographs (*n* = 10) of mitochondrial nascent proteins in situ. Mouse C2C12 cells were incubated with HPG in the presence or absence of inhibitors (ANS and CAP). HPG-labeled proteins were visualized with Cy3. Mitochondria and nuclei were stained with MitoTracker Deep Red and DAPI, respectively. (*D*) Representative micrographs of mitochondrial nascent proteins in the indicated human cell lines (HEK293, *n* = 9; HeLa S3, *n* = 4). HPG-labeled proteins were visualized with Cy3. Mitochondria were stained with MitoTracker. In *C* and *D*, the scale bar represents 15 μm.

Indeed, mito-FUNCAT-FACS on C2C12 cells (Supplemental Fig. 4A) successfully distinguished the signal of HPGylated mitochondrial nascent proteins (Fig. 2B +HPG +ANS) from the background (Fig. 2B −HPG). Reduction of the signal with CAP (Fig. 2B +HPG +ANS +CAP) further ensured the detection of mitochondrial translation products.

Since FACS allows us to track multiple fluorescent markers, we simultaneously measured mitochondrial abundance by translocase of outer mitochondrial membrane 20 (TOM20)— a receptor of presequence-carrying preproteins (Wiedemann and Pfanner 2017)—by immunostaining with a different fluorescent profile than the one used for the mitochondrial nascent peptides. This enabled the normalization of the mito-FUNCAT signal variation caused by differential mitochondrial masses in cells (Fig. 2C,D) and refined the resolution of mitochondrial translation measurements (Fig. 2E). Similar normalization can be conducted using MitoTracker Deep Red (Supplemental Figs. S2, S4B; Agnello et al. 2008; Cottet-Rousselle et al. 2011; Yeung et al. 2015), although staining with this dye depends on the membrane potential.

Mitochondrial function-associated translation activation monitored by mito-FUNCAT-FACS

To confirm the performance of mito-FUNCAT-FACS, we observed alterations in mitochondrial translation during organelle biogenesis. For this purpose, HeLa S3 cells were treated with bezafibrate, a peroxisome proliferator-activated receptor (PPAR) panagonist, which causes increased mitochondrial biogenesis and, thus, an increased number of OXPHOS complexes (Bastin et al. 2008; Wang and Moraes 2011; Wenz et al. 2011). An earlier work using L-[35S]-methionine metabolic labeling (Wenz et al. 2011) showed that bezafibrate may increase mitochondrial translation. Similarly, our on-gel mito-FUNCAT reproduced the elevated mitochondrial protein synthesis observed with bezafibrate treatment (Fig. 3A). However, irrespective of the methods (L-[35S]-methionine or HPG), these data could not distinguish whether the enhanced protein synthesis originated from an increased
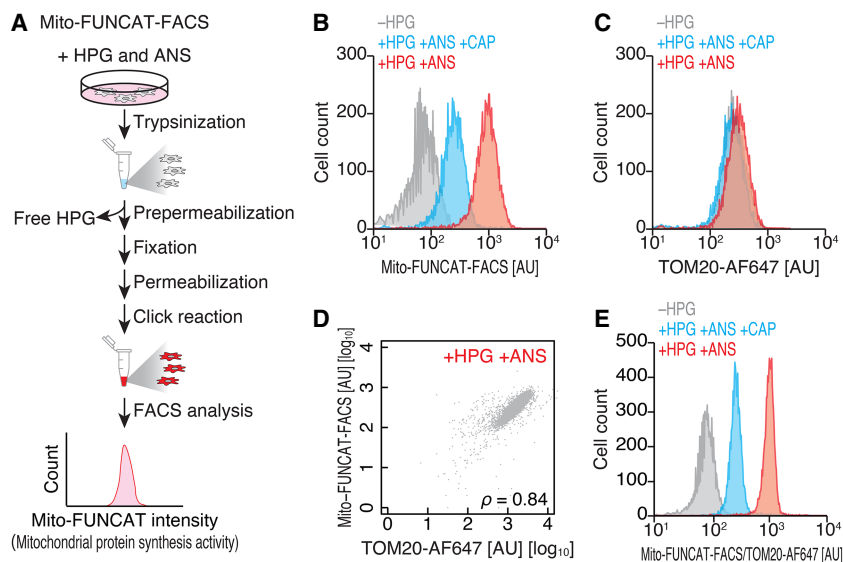
and FACS assays) than earlier reports (Estell et al. 2017; Yousefi et al. 2021; Zorkau et al. 2021) (0.5–1 mM) to prevent the introduction of biases and/or artifacts with high doses of this compound. Under these conditions, we observed incremental accumulation of newly synthesized proteins in mitochondria over time (Supplemental Fig. S1F). Given the sufficiently high signal, we used a 3-h incubation condition throughout the experiments in this study.

Implementation of mito-FUNCAT for FACS analysis

Next, we adapted the in situ mito-FUNCAT approach for use with flow cytometry (mito-FUNCAT-FACS) (Fig. 2A).

FIGURE 2. FACS-based quantification of mito-FUNCAT (mito-FUNCAT-FACS). (*A*) Schematic representation of the mito-FUNCAT-FACS procedure. (*B,C*) Representative distribution (*n* = 4) of Cy3-conjugated HPG signals (*B*, mito-FUNCAT-FACS) and Alexa Fluor (AF) 647-labeled TOM20 signals (*C*) across C2C12 cells in FACS. Cells were analyzed in the presence or absence of translation inhibitors (ANS and CAP) and HPG. Data from 1 × 10⁴ cells are shown. (*D*) Scatter plot for Cy3-conjugated HPG signals and AF647-labeled TOM20 signals across cells analyzed in *B* and *C*. ρ, Spearman's rank correlation coefficient. (*E*) The distribution of mito-FUNCAT-FACS signals (in *B*) normalized to the AF647-labeled TOM20 intensity (in *C*). (AU) Arbitrary unit.

nocarcinoma, whereas H441 cells do not. It is commonly believed that the loss of *LKB1* and *KEAP1* leads to enhanced tricarboxylic acid (TCA) cycle flux (Faubert et al. 2014) and maintains a high mitochondrial biosynthetic capacity (Kottakis et al. 2016). Consistent with the enhanced mitochondrial functions, the averaged signals of mito-FUNCAT-FACS in H2122 cells tended to be higher than those in H441 cells (Fig. 3E; Supplemental Fig. 4E). The increased mitochondrial translation occurred beyond the abundance of the organelle mass (Fig. 3F,G), suggesting that H2122 cells used the increased mitochondrial translation to increase biosynthesis in the organelle.

Mito-FUNCAT-FACS reveals heterogeneity of mitochondrial protein synthesis in cancer cells

In addition to utilizing averaged measurements, flow cytometry is useful for assessing cell subpopulations. We used mito-FUNCAT-FACS to survey cellular heterogeneity in mitochondrial translation in various cell lines (C2C12, HeLa S3, HEK293T, A375, H441, H1944, H2009, and H2122) (Fig. 4A; Supplemental Fig. 4A–F). Indeed, we observed that H2009, H441, and H2122 cells showed a wide range of mitochondrial translation activity (Fig. 4A). The heterogeneity in H2122 cells was also evident from the in situ mito-FUNCAT data, which highlighted a subset of cells exhibiting a relatively high capacity for mitochondrial protein synthesis (Fig. 4B) (note that this in situ mito-FUNCAT was conducted with TOM20 immunostaining instead of MitoTracker staining for the assessment of mitochondria as shown in Fig. 1C,D). This phenotype was in contrast to C2C12 cells, which showed relatively uniform mitochondrial translation both in FACS and in situ microscopic options of mito-FUNCAT (Fig. 4A,B). The subpopulation of H2122 cells with high mitochondrial translation was associated with lower cell size and internal complexity, as indicated by forward and side scatter (FSC and SSC), suggesting unique characteristics of the cell population (Fig. 4C).

Thus, mito-FUNCAT-FACS developed in this work provides a useful framework for unveiling the previously-overlooked heterogeneity in mitochondrial protein synthesis among cell populations. These previously unreported differences in mitochondrial translation in H2122 cells (Fig. 4) need further study to develop detailed characterizations. Given the ability of this technique to perform cell sorting
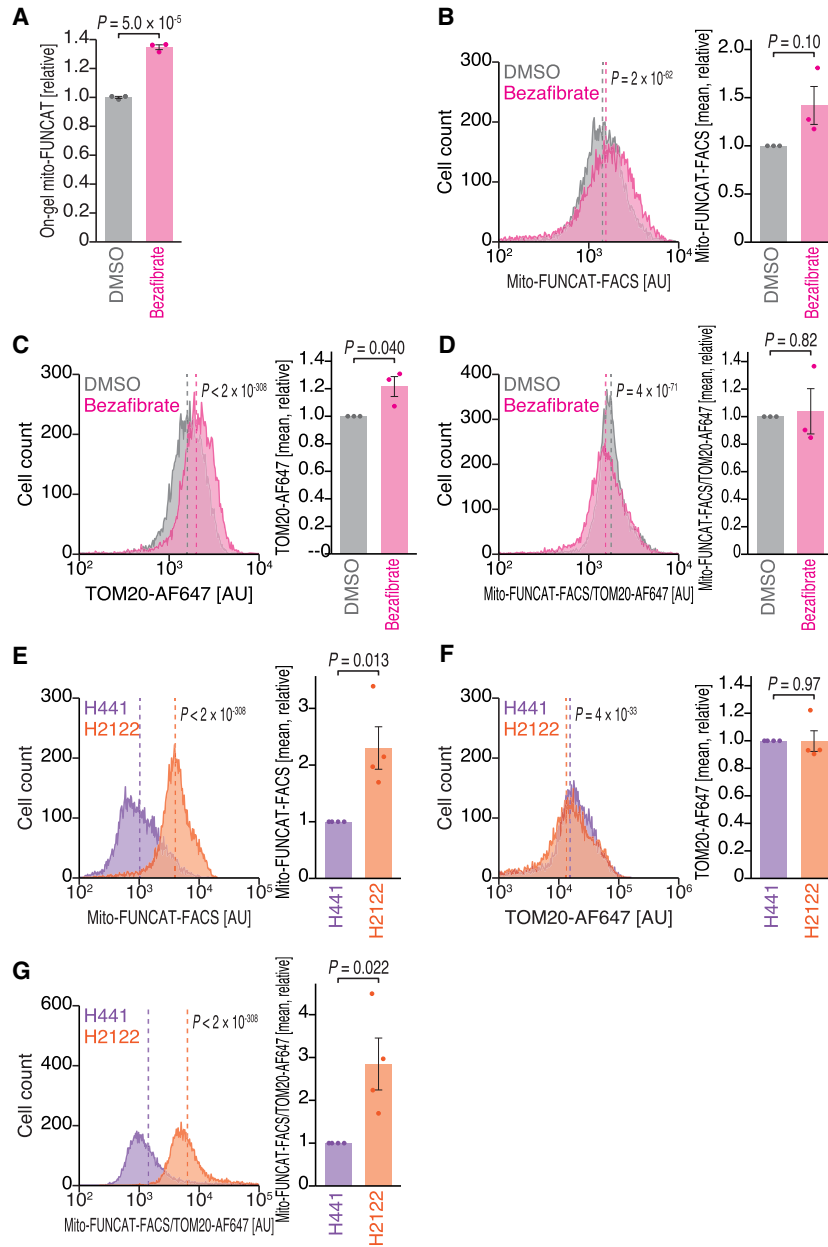
abundance of mitochondria or increased translation in the organelle.

Thus, we applied mito-FUNCAT-FACS and normalized the signals of HPGylated proteins according to the mitochondrial abundance measured via TOM20. The raw signals from HPGylated nascent peptides showed an increase with bezafibrate treatment (Fig. 3B; Supplemental Fig. 4C), consistent with on-gel mito-FUNCAT (Fig. 3A). However, we observed a simultaneous increase in mitochondrial mass by TOM20 immunostaining (Fig. 3C). Normalization of the mito-FUNCAT-FACS signals to the mitochondrial mass reduced the scores (Fig. 3D), indicating that the bezafibrate-mediated increase in HPGylated proteins in mitochondria resulted from the increased organelle mass but not from a net increase in translation. Similar results were obtained from MitoTracker normalization (Supplemental Figs. S3, S4D). These data exemplified the ability of our FACS-based approach to disentangle the effects of mitochondrial translation and organelle biogenesis in individual cells.

To further evaluate the potential of mito-FUNCAT-FACS, we compared in organello translation in two different types of *KRAS* (Kirsten rat sarcoma viral oncogene homolog)-mutated lung cancer cell lines, H2122 and H441. H2122 cells possess mutations in the liver kinase B1 (*LKB1*) gene (also called the serine/threonine kinase 11 [*STK11*]) and Kelch-like ECH-associated protein 1 (*KEAP1*) gene, which are common mutations in lung ade-

FIGURE 3. Mitochondrial protein synthesis under bezafibrate treatment assessed by mito-FUNCAT-FACS. (*A*) Bulk mitochondrial translation changes in HeLa S3 cells upon bezafibrate treatment, analyzed via on-gel mito-FUNCAT. Data from three replicates (points) and the mean (bar) with SD (error bar) are shown. (*B,C*) Representative distribution (*n* = 3) of Cy3-conjugated HPG signals (*B*, mito-FUNCAT-FACS) and AF647-labeled TOM20 signals (*C*) across HeLa S3 cells with or without bezafibrate treatment, analyzed by FACS. Data from 1×10^4 cells are shown. The dashed line indicates the mean of the distribution. Significance was determined by the Mann–Whitney *U*-test (two-tailed). In the bar graphs, data from three replicates (mean of 1×10^4 cells, relative to DMSO treatment) (points) and the mean (bar) with SD (error bar) are shown, and significance was determined by Tukey's test. (*D*) The distribution of mito-FUNCAT-FACS signals (in *B*) normalized to the AF647-labeled TOM20 intensity (in *C*). Significance was determined by the Mann–Whitney *U*-test (two-tailed). The dashed line indicates the mean of the distribution. In the bar graphs, data from three replicates (mean of 1×10^4 cells, relative to DMSO treatment) (points) and the mean (bar) with SD (error bar) are shown, and significance was determined by Tukey's test. (*E–G*) The same as *B–D* but comparing H441 and H2122 cells. Representative data (*n* = 4) are shown. (AU) Arbitrary unit.

and isolation, the assessment of gene expression profiles by bulk RNA-seq and single-cell RNA-seq can address the mechanism underlying the variation in mitochondrial translation. Application of this experimental setup will pave the way for elucidating the in organello translation heterogeneity across a wide array of cell types, developmental stages, and responses to internal/external stimuli.
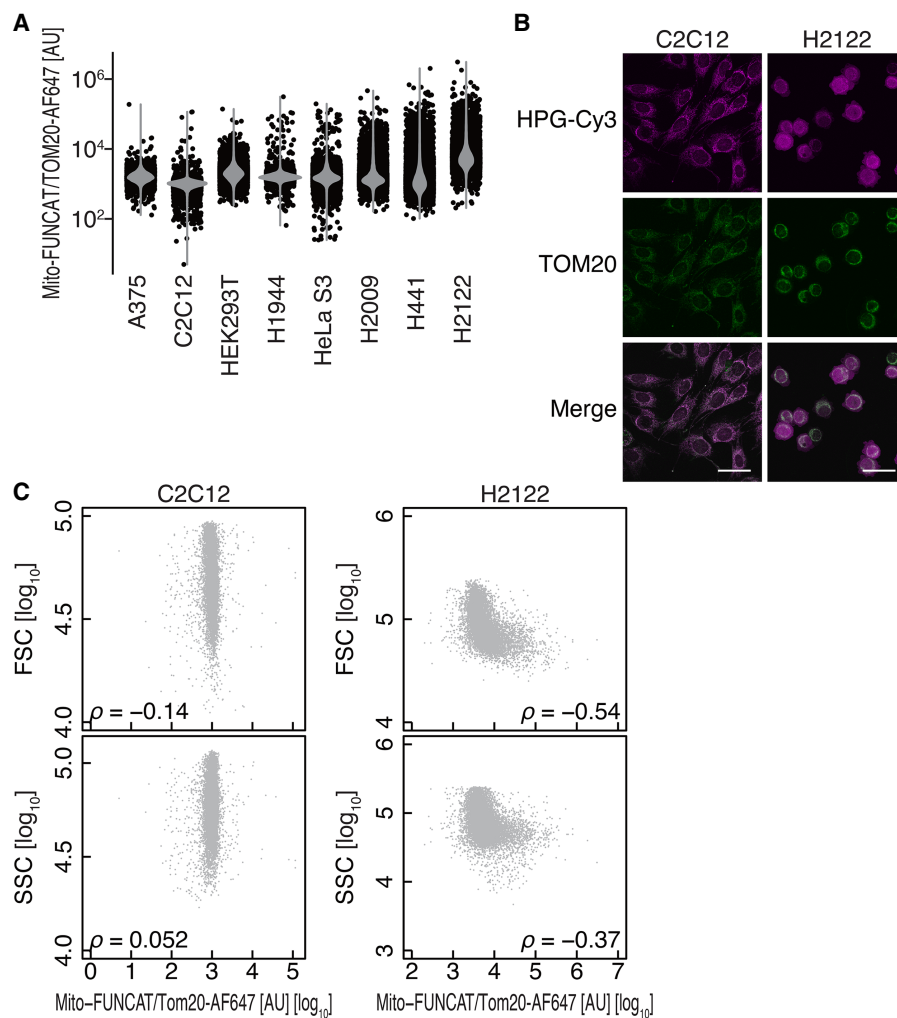
FIGURE 4. Heterogeneity of mitochondrial protein synthesis in H2122 cells. (*A*) Distributions of mito-FUNCAT-FACS scores (normalized to the AF647-labeled TOM20 intensity) in the indicated cell lines. Data from 1×10^4 cells are shown. (*B*) Representative micrographs (*n* = 2) of mitochondrial nascent proteins detected by in situ mito-FUNCAT (Cy3-conjugated HPG). Mouse C2C12 and human H2122 cells were analyzed. Mitochondria were stained with anti-TOM20 antibodies. Since the subpopulation of H2122 cells showed a relatively weaker HPG-Cy3 signal, imaging required a higher intensity of laser power, which may cause a higher background signal (such as in the nucleus). Notably, even with the higher laser power, images were acquired to avoid signal saturation. The scale bar represents 50 µm. (*C*) Scatter plots of mito-FUNCAT-FACS scores (TOM20-normalized) and forward scatter (FSC) or side scatter (SSC) in C2C12 and H2122 cells. ρ, Spearman's rank correlation coefficient. (AU) Arbitrary unit.

MATERIALS AND METHODS

Cell culture

Cells were maintained in the following culture medium: C2C12 (mouse myoblast, American Type Culture Collection [ATCC], CRL-1772), HeLa S3 (RIKEN BioResource Research Center, RCB1525), HEK293 (human embryonic kidney, ATCC, CRL-1573), HEK293T (ATCC, CRL-3216), A375 (human malignant melanoma, ATCC, CRL-1619), and H2009 (human lung adenocarcinoma, ATCC, CRL-5911) cells were maintained in DMEM, high glucose, GlutaMAX supplement (Thermo Fisher Scientific, 10566016) with 10% fetal bovine serum (FBS); H2122 (human lung adenocarcinoma, ATCC, CRL-5985), H1944 (human lung adenocarcinoma, ATCC, CRL-5907), and H441 (human lung adenocarcinoma, ATCC,

HTB-174) cells were maintained in RPMI 1640 medium (Thermo Fisher Scientific, A1049101) with 10% FBS and 1% penicillin-streptomycin (Thermo Fisher Scientific, 15140148). All cells were cultured in a humidified incubator under 5% CO_2 at 37°C.

The following compounds were used in this study: ANS (ChemImpex International), CAP (FUJIFILM Wako Pure Chemical Corporation), CHX (Sigma-Aldrich), EME (Cayman Chemical), and bezafibrate (FUJIFILM Wako Pure Chemical Corporation).

On-gel mito-FUNCAT

Cells were washed with PBS and incubated in methionine-free DMEM with 50 µM HPG (Jena Bioscience) and 100 µg/mL ANS, CHX, or EME for 3 h. For mitochondrial translation inhibition,

100 µg/mL CAP was added to the medium. Then, the cells were washed with ice-cold PBS and lysed with lysis buffer (20 mM Tris-HCl pH 7.5, 150 mM NaCl, 5 mM MgCl$_2$, and 1% Triton X-100). The lysate was cleared by centrifugation at 20,000g at 4°C for 10 min. The supernatant was used for the click reaction with 50 µM azide-IRDye800CW (LI-COR Biosciences) by a Click-iT Cell Reaction Buffer Kit (Thermo Fisher Scientific) according to the manufacturer's instructions, followed by SDS-PAGE. Images of labeled nascent peptides were acquired with an Odyssey CLx Infrared Imaging System (LI-COR Biosciences) in the 800 nm channel. Subsequently, the gel was stained with Coomassie brilliant blue (CBB) using EzStain AQua (ATTO) and imaged in the 700 nm channel to measure the protein input. The images were quantified with Image Studio version 5.2 (LI-COR Biosciences).

For mitochondrial isolation, EzSubcell Fraction (ATTO) was used according to the manufacturer's instructions. The purified mitochondria were lysed with lysis buffer.

For AHA-mediated mito-FUNCAT, AHA (Thermo Fisher Scientific) and alkyne-IRDye800CW (LI-COR Biosciences) were used instead of HPG and azide-IRDye800CW, respectively.

In situ mito-FUNCAT

Typically, 2×10^4 cells were cultured on a laminin-coated Lab-Tek II Chamber Slide (Thermo Fisher Scientific) in 200 µL of methionine-free DMEM with 100 µM HPG and 100 µg/mL ANS. For mitochondrial translation inhibition, 100 µg/mL CAP was added to the medium. Cells were washed with 200 µL of prewarmed PBS, prepermeabilized with 0.0005% digitonin in 200 µL of mitochondrial protective buffer (10 mM HEPES-KOH pH 7.5, 300 mM sucrose, 10 mM NaCl, and 5 mM MgCl$_2$) for 5 min, and fixed in 200 µL of 4% paraformaldehyde (PFA) for 15 min. Then, the cells were fully permeabilized with 0.1% (v/v) Triton X-100 in 200 µL of PBS for 5 min and subsequently incubated in 100 µL of click reaction buffer (1× Click-iT cell reaction buffer [Thermo Fisher Scientific], 2 mM CuSO$_4$, 1× Click-iT cell buffer additive [Thermo Fisher Scientific], and 1 µM azide-conjugated Cy3 [(Jena Bioscience)] for 30 min according to the Click-iT Cell Reaction Buffer Kit (Thermo Fisher Scientific) to label nascent proteins via the click reaction. After washing with 200 µL of Intercept Blocking Buffer (LI-COR Biosciences), mitochondria were immunostained in 100 µL of Intercept Blocking Buffer containing 1 µL of Alexa Fluor 647 Anti-TOM20 antibody (Abcam, ab209606) for 1 h at 4°C. The cells were washed with 200 µL of PBS twice, and then the nuclei were stained with 4′,6-diamidino-2-phenylindole (DAPI) (Thermo Fisher Scientific) for 5 min. Images were obtained using an FV3000 confocal microscope (Olympus) with a 60× objective lens (Olympus Japan, UPLSAPO60XS2).

For C2C12 and HeLa S3 cells, mitochondria were stained with 100 nM MitoTracker Deep Red FM (Thermo Fisher Scientific) for 15 min during HPG labeling, omitting TOM20 immunostaining.

Images were colored by standard look-up tables (LUTs) in FV3000 software and exported in TIF format (24 bit). ImageJ2 (https://github.com/imagej/imagej2, version 2.3.0) was used to overlay images.

Mito-FUNCAT-FACS

Cells were handled as described in the "In situ mito-*FUNCAT*" section with some modifications. Approximately 1×10^6 cells were cultured in a 10-cm dish with 10 mL of methionine-free DMEM with 100 µM HPG and 100 µg/mL ANS. Then, the cells were washed with 5 mL of PBS, trypsinized with 1.5 mL of 0.05% trypsin-EDTA (Thermo Fisher Scientific), collected into 2.0-mL tubes, and washed with 500 µL of PBS. Prepermeabilization, fixation, permeabilization, click reaction, and immunostaining were conducted in a 2.0-mL tube as described in "In situ mito-*FUNCAT*," using 500 µL of mitochondrial protective buffer with 0.0005% digitonin, 500 µL of 4% PFA, 500 µL of 0.1% (v/v) Triton X-100 in PBS, 250 µL of click reaction buffer, and 100 µL of Intercept Blocking Buffer containing 1 µL of Alexa Fluor 647 Anti-TOM20 antibody, respectively. Cells were collected by centrifugation at 300g for 3 min before fixation and by centrifugation at 1000g for 3 min after fixation. Cells were analyzed with a FACSAria II cell sorter or FACSMelody (BD Biosciences). Data from 1×10^4 cells are depicted in the graphs.

SUPPLEMENTAL MATERIAL

Supplemental material is available for this article.

ACKNOWLEDGMENTS

REFERENCES

Agnello M, Morici G, Rinaldi AM. 2008. A method for measuring mitochondrial mass and activity. *Cytotechnology* **56:** 145–149. doi:10.1007/s10616-008-9143-2

Ali TH, Heidelberg T, Hussen RSD, Tajuddin HA. 2019. Unexpected reactions of terminal alkynes in targeted "Click chemistry" coppercatalyzed azide-alkyne cycloadditions. *Curr Org Synth* **16:** 1143–1148. doi:10.2174/1570179416666191105152714

Anderson S, Bankier AT, Barrell BG, de Bruijn MH, Coulson AR, Drouin J, Eperon IC, Nierlich DP, Roe BA, Sanger F, et al. 1981. Sequence and organization of the human mitochondrial genome. *Nature* **290:** 457–465. doi:10.1038/290457a0

Antonicka H, Sasarman F, Nishimura T, Paupe V, Shoubridge EA. 2013. The mitochondrial RNA-binding protein GRSF1 localizes to RNA granules and is required for posttranscriptional mitochondrial gene expression. *Cell Metab* **17:** 386–398. doi:10.1016/j.cmet.2013.02.006

Asano K, Suzuki T, Saito A, Wei F-Y, Ikeuchi Y, Numata T, Tanaka R, Yamane Y, Yamamoto T, Goto T, et al. 2018. Metabolic and chemical regulation of tRNA modification associated with taurine deficiency and human disease. *Nucleic Acids Res* **46:** 1565–1583. doi:10.1093/nar/gky068

Bastin J, Aubey F, Rötig A, Munnich A, Djouadi F. 2008. Activation of peroxisome proliferator-activated receptor pathway stimulates the mitochondrial respiratory chain and can correct deficiencies in patients' cells lacking its components. *J Clin Endocrinol Metab* **93:** 1433–1441. doi:10.1210/jc.2007-1701

Beatty KE, Tirrell DA. 2008. Two-color labeling of temporally defined protein populations in mammalian cells. *Bioorg Med Chem Lett* **18:** 5995–5999. doi:10.1016/j.bmcl.2008.08.046

Beatty KE, Liu JC, Xie F, Dieterich DC, Schuman EM, Wang Q, Tirrell DA. 2006. Fluorescence visualization of newly synthesized proteins in mammalian cells. *Angew Chem Int Ed Engl* **45:** 7364–7367. doi:10.1002/anie.200602114

Cahoon AB, Qureshi AA. 2018. Leaderless mRNAs are circularized in *Chlamydomonas reinhardtii* mitochondria. *Curr Genet* **64:** 1321–1333. doi:10.1007/s00294-018-0848-2

Cottet-Rousselle C, Ronot X, Leverve X, Mayol JF. 2011. Cytometric assessment of mitochondria using fluorescent probes. *Cytometry A* **79:** 405–425. doi:10.1002/cyto.a.21061

Couvillion MT, Churchman LS. 2017. Mitochondrial ribosome (mitoribosome) profiling for monitoring mitochondrial translation in vivo. *Curr Protoc Mol Biol* **119:** 4.28.1–4.28.25. doi:10.1002/cpmb.41

Couvillion MT, Soto IC, Shipkovenska G, Churchman LS. 2016. Synchronized mitochondrial and cytosolic translation programs. *Nature* **533:** 499–503. doi:10.1038/nature18015

Cruz-Zaragoza LD, Dennerlein S, Linden A, Yousefi R, Lavdovskaia E, Aich A, Falk RR, Gomkale R, Schöndorf T, Bohnsack MT, et al. 2021. An *in vitro* system to silence mitochondrial gene expression. *Cell* **184:** 5824–5837.e15. doi:10.1016/j.cell.2021.09.033

De Silva D, Tu Y-T, Amunts A, Fontanesi F, Barrientos A. 2015. Mitochondrial ribosome assembly in health and disease. *Cell Cycle* **14:** 2226–2250. doi:10.1080/15384101.2015.1053672

Dieterich DC, Hodas JJ, Gouzer G, Shadrin IY, Ngo JT, Triller A, Tirrell DA, Schuman EM. 2010. *In situ* visualization and dynamics of newly synthesized proteins in rat hippocampal neurons. *Nat Neurosci* **13:** 897–905. doi:10.1038/nn.2580

Dunkle JA, Xiong L, Mankin AS, Cate JH. 2010. Structures of the *Escherichia coli* ribosome with antibiotics bound near the peptidyl transferase center explain spectra of drug action. *Proc Natl Acad Sci* **107:** 17152–17157. doi:10.1073/pnas.1007988107

Englmeier R, Pfeffer S, Förster F. 2017. Structure of the human mitochondrial ribosome studied *in situ* by cryoelectron tomography. *Structure* **25:** 1574–1581.e2. doi:10.1016/j.str.2017.07.011

Estell C, Stamatidou E, El-Messeiry S, Hamilton A. 2017. *In situ* imaging of mitochondrial translation shows weak correlation with nucleoid DNA intensity and no suppression during mitosis. *J Cell Sci* **130:** 4193–4199. doi:10.1242/jcs.206714

Faubert B, Vincent EE, Griss T, Samborska B, Izreig S, Svensson RU, Mamer OA, Avizonis D, Shackelford DB, Shaw RJ, et al. 2014. Loss of the tumor suppressor LKB1 promotes metabolic reprogramming of cancer cells via HIF-1α. *Proc Natl Acad Sci* **111:** 2554–2559. doi:10.1073/pnas.1312570111

Fung S, Nishimura T, Sasarman F, Shoubridge EA. 2013. The conserved interaction of C7orf30 with MRPL14 promotes biogenesis of the mitochondrial large ribosomal subunit and mitochondrial translation. *Mol Biol Cell* **24:** 184–193. doi:10.1091/mbc.e12-09-0651

Gao F, Wesolowska M, Agami R, Rooijers K, Loayza-Puch F, Lawless C, Lightowlers RN, Chrzanowska-Lightowlers ZMA. 2017. Using mitoribosomal profiling to investigate human mitochondrial translation. *Wellcome Open Res* **2:** 116. doi:10.12688/wellcomeopenres.13119.1

Garreau de Loubresse N, Prokhorova I, Holtkamp W, Rodnina MV, Yusupova G, Yusupov M. 2014. Structural basis for the inhibition of the eukaryotic ribosome. *Nature* **513:** 517–522. doi:10.1038/nature13737

Grimes BT, Sisay AK, Carroll HD, Cahoon AB. 2014. Deep sequencing of the tobacco mitochondrial transcriptome reveals expressed ORFs and numerous editing sites outside coding regions. *BMC Genomics* **15:** 31. doi:10.1186/1471-2164-15-31

Grivell LA, Reijnders L, de Vries H. 1971. Altered mitochondrial ribosomes in a cytoplasmic mutant of yeast. *FEBS Lett* **16:** 159–163. doi:10.1016/0014-5793(71)80121-7

Hinz FI, Dieterich DC, Tirrell DA, Schuman EM. 2012. Non-canonical amino acid labeling *in vivo* to visualize and affinity purify newly synthesized proteins in larval zebrafish. *ACS Chem Neurosci* **3:** 40–49. doi:10.1021/cn2000876

Imami K, Selbach M, Ishihama Y. 2021. Monitoring mitochondrial translation by pulse SILAC. bioRxiv doi:10.1101/2021.01.31.428997

Ingolia NT, Ghaemmaghami S, Newman JR, Weissman JS. 2009. Genome-wide analysis *in vivo* of translation with nucleotide resolution using ribosome profiling. *Science* **324:** 218–223. doi:10.1126/science.1168978

Iwasaki S, Ingolia NT. 2017. The growing toolbox for protein synthesis studies. *Trends Biochem Sci* **42:** 612–624. doi:10.1016/j.tibs.2017.05.004

Iwasaki S, Floor SN, Ingolia NT. 2016. Rocaglates convert DEAD-box protein eIF4A into a sequence-selective translational repressor. *Nature* **534:** 558–561. doi:10.1038/nature17978

Jeffreys AJ, Craig IW. 1976. Analysis of proteins synthesized in mitochondria of cultured mammalian cells. An assessment of current approaches and problems in interpretation. *Eur J Biochem* **68:** 301–311. doi:10.1111/j.1432-1033.1976.tb10789.x

Kashiwagi K, Shichino Y, Osaki T, Sakamoto A, Nishimoto M, Takahashi M, Mito M, Weber F, Ikeuchi Y, Iwasaki S, et al. 2021. eIF2B-capturing viral protein NSs suppresses the integrated stress response. *Nat Commun* **12:** 1–12. doi:10.1038/s41467-021-27337-x

Keilland E, Rupar CA, Prasad AN, Tay KY, Downie A, Prasad C. 2016. The expanding phenotype of MELAS caused by the m.3291T>C mutation in the MT-TL1 gene. *Mol Genet Metab Rep* **6:** 64–69. doi:10.1016/j.ymgmr.2016.02.003

Kirino Y, Goto Y-I, Campos Y, Arenas J, Suzuki T. 2005. Specific correlation between the wobble modification deficiency in mutant tRNAs and the clinical features of a human mitochondrial disease. *Proc Natl Acad Sci* **102:** 7127–7132. doi:10.1073/pnas.0500563102

Kottakis F, Nicolay BN, Roumane A, Karnik R, Gu H, Nagle JM, Boukhali M, Hayward MC, Li YY, Chen T, et al. 2016. LKB1 loss links serine metabolism to DNA methylation and tumorigenesis. *Nature* **539:** 390–395. doi:10.1038/nature20132

Kummer E, Ban N. 2021. Mechanisms and regulation of protein synthesis in mitochondria. *Nat Rev Mol Cell Biol* **22:** 307–325. doi:10.1038/s41580-021-00332-2

Lee M, Matsunaga N, Akabane S, Yasuda I, Ueda T, Takeuchi-Tomita N. 2021. Reconstitution of mammalian mitochondrial translation system capable of correct initiation and long polypeptide synthesis from leaderless mRNA. *Nucleic Acids Res* **49:** 371–382. doi:10.1093/nar/gkaa1165

Li SH-J, Nofal M, Parsons LR, Rabinowitz JD, Gitai Z. 2021. Monitoring mammalian mitochondrial translation with MitoRiboSeq. *Nat Protoc* **16:** 2802–2825. doi:10.1038/s41596-021-00517-1

Morscher RJ, Ducker GS, Li SH-J, Mayer JA, Gitai Z, Sperl W, Rabinowitz JD. 2018. Mitochondrial translation requires folate-dependent tRNA methylation. *Nature* **554:** 128–132. doi:10.1038/nature25460

Pearce SF, Rorbach J, Van Haute L, D'Souza AR, Rebelo-Guiomar P, Powell CA, Brierley I, Firth AE, Minczuk M. 2017. Maturation of selected human mitochondrial tRNAs requires deadenylation. *Elife* **6:** e27596. doi:10.7554/eLife.27596

Pfeffer S, Woellhaf MW, Herrmann JM, Förster F. 2015. Organization of the mitochondrial translation machinery studied *in situ* by cryoelectron tomography. *Nat Commun* **6:** 6019. doi:10.1038/ncomms7019

Roche FK, Marsick BM, Letourneau PC. 2009. Protein synthesis in distal axons is not required for growth cone responses to guidance cues. *J Neurosci* **29:** 638–652. doi:10.1523/JNEUROSCI.3845-08.2009

Rooijers K, Loayza-Puch F, Nijtmans LG, Agami R. 2013. Ribosome profiling reveals features of normal and disease-associated mitochondrial translation. *Nat Commun* **4:** 2886. doi:10.1038/ncomms3886

Rötig A. 2011. Human diseases with impaired mitochondrial protein synthesis. *Biochim Biophys Acta* **1807:** 1198–1205. doi:10.1016/j.bbabio.2011.06.010

Scharfe C, Lu HH-S, Neuenburg JK, Allen EA, Li G-C, Klopstock T, Cowan TM, Enns GM, Davis RW. 2009. Mapping gene associations in human mitochondria using clinical disease phenotypes. *PLoS Comput Biol* **5:** e1000374. doi:10.1371/journal.pcbi.1000374

Schöller E, Marks J, Marchand V, Bruckmann A, Powell CA, Reichold M, Mutti CD, Dettmer K, Federle R, Hüttelmaier S, et al. 2021. Balancing of mitochondrial translation through METTL8-mediated m^{3}C modification of mitochondrial tRNAs. *Mol Cell* **81:** 4810–4825.e12. doi:10.1016/j.molcel.2021.10.018

Signer RA, Magee JA, Salic A, Morrison SJ. 2014. Haematopoietic stem cells require a highly regulated protein synthesis rate. *Nature* **509:** 49–54. doi:10.1038/nature13035

Speers AE, Cravatt BF. 2004. Profiling enzyme activities in vivo using click chemistry methods. *Chem Biol* **11:** 535–546. doi:10.1016/j.chembiol.2004.03.012

Suomalainen A, Battersby BJ. 2018. Mitochondrial diseases: the contribution of organelle stress responses to pathology. *Nat Rev Mol Cell Biol* **19:** 77–92. doi:10.1038/nrm.2017.66

Suzuki T, Yashiro Y, Kikuchi I, Ishigami Y, Saito H, Matsuzawa I, Okada S, Mito M, Iwasaki S, Ma D, et al. 2020. Complete chemical structures of human mitochondrial tRNAs. *Nat Commun* **11:** 4269. doi:10.1038/s41467-020-18068-6

Tcherkezian J, Brittis PA, Thomas F, Roux PP, Flanagan JG. 2010. Transmembrane receptor DCC associates with protein synthesis machinery and regulates translation. *Cell* **141:** 632–644. doi:10.1016/j.cell.2010.04.008

Wang X, Moraes CT. 2011. Increases in mitochondrial biogenesis impair carcinogenesis at multiple levels. *Mol Oncol* **5:** 399–409. doi:10.1016/j.molonc.2011.07.008

Webb BD, Diaz GA, Prasun P. 2020. Mitochondrial translation defects and human disease. *J Transl Genet Genom* **4:** 71–80. doi:10.20517/jtgg.2020.11

Wenz T, Wang X, Marini M, Moraes CT. 2011. A metabolic shift induced by a PPAR panagonist markedly reduces the effects of pathogenic mitochondrial tRNA mutations. *J Cell Mol Med* **15:** 2317–2325. doi:10.1111/j.1582-4934.2010.01223.x

Weraarpachai W, Antonicka H, Sasarman F, Seeger J, Schrank B, Kolesar JE, Lochmüller H, Chevrette M, Kaufman BA, Horvath R, et al. 2009. Mutation in *TACO1*, encoding a translational activator of COX I, results in cytochrome *c* oxidase deficiency and late-onset Leigh syndrome. *Nat Genet* **41:** 833–837. doi:10.1038/ng.390

Wiedemann N, Pfanner N. 2017. Mitochondrial machineries for protein import and assembly. *Annu Rev Biochem* **86:** 685–714. doi:10.1146/annurev-biochem-060815-014352

Wong W, Bai X-C, Brown A, Fernandez IS, Hanssen E, Condron M, Tan YH, Baum J, Scheres SHW. 2014. Cryo-EM structure of the *Plasmodium falciparum* 80S ribosome bound to the anti-protozoan drug emetine. *Elife* **3:** e03080. doi:10.7554/eLife.03080

Yasukawa T, Suzuki T, Ishii N, Ueda T, Ohta S, Watanabe K. 2000a. Defect in modification at the anticodon wobble nucleotide of mitochondrial tRNA^{Lys} with the MERRF encephalomyopathy pathogenic mutation. *FEBS Lett* **467:** 175–178. doi:10.1016/S0014-5793(00)01145-5

Yasukawa T, Suzuki T, Suzuki T, Ueda T, Ohta S, Watanabe K. 2000b. Modification defect at anticodon wobble nucleotide of mitochondrial tRNAs^{Leu} (UUR) with pathogenic mutations of mitochondrial myopathy, encephalopathy, lactic acidosis, and stroke-like episodes. *J Biol Chem* **275:** 4251–4257. doi:10.1074/jbc.275.6.4251

Yeung M, Hurren R, Nemr C, Wang X, Hershenfeld S, Gronda M, Liyanage S, Wu Y, Augustine J, Lee EA, et al. 2015. Mitochondrial DNA damage by bleomycin induces AML cell death. *Apoptosis* **20:** 811–820. doi:10.1007/s10495-015-1119-z

Yoon BC, Jung H, Dwivedy A, O'Hare CM, Zivraj KH, Holt CE. 2012. Local translation of extranuclear lamin B promotes axon maintenance. *Cell* **148:** 752–764. doi:10.1016/j.cell.2011.11.064

Yousefi R, Fornasiero EF, Cyganek L, Montoya J, Jakobs S, Rizzoli SO, Rehling P, Pacheu-Grau D. 2021. Monitoring mitochondrial translation in living cells. *EMBO Rep* **22:** e51635. doi:10.15252/embr.202051635

Zhang X, Zuo X, Yang B, Li Z, Xue Y, Zhou Y, Huang J, Zhao X, Zhou J, Yan Y, et al. 2014. MicroRNA directly enhances mitochondrial translation during muscle differentiation. *Cell* **158:** 607–619. doi:10.1016/j.cell.2014.05.047

Zorkau M, Albus CA, Berlinguer-Palmini R, Chrzanowska-Lightowlers ZMA, Lightowlers RN. 2021. High-resolution imaging reveals compartmentalization of mitochondrial protein synthesis in cultured human cells. *Proc Natl Acad Sci* **118:** e2008778118. doi:10.1073/pnas.2008778118

*See the following page for **Meet the First Authors***

MEET THE FIRST AUTHORS

Yusuke Kimura

Hironori Saito

Meet the First Author(s) is a new editorial feature within RNA, *in which the first author(s) of research-based papers in each issue have the opportunity to introduce themselves and their work to readers of* RNA *and the RNA research community. Yusuke Kimura and Hironori Saito are the co-first authors of this paper, "Mito-FUNCAT-FACS reveals cellular heterogeneity in mitochondrial translation." Yusuke and Hironori did this work as PhD students at the The University of Tokyo under the supervision of Dr. Shintaro Iwasaki (RIKEN), focusing on the regulation of* in organello *translation.*

What are the major results described in your paper and how do they impact this branch of the field?

Mito-FUNCAT-FACS, which we developed in this study, enables high-throughput detection of mitochondrial translation activity in cells. We believe that this technique could be applicable for varieties of cell types and provides a useful platform to survey protein synthesis in the organella.

What led you to study RNA or this aspect of RNA science?

Y.K.: Given the earlier reports that revealed the diversity of cytosolic translation among cells, we wondered if mitochondrial translation is regulated in different types of cells as well. To test that, we started developing a new method, mito-FUNCAT-FACS.

During the course of these experiments, were there any surprising results or particular difficulties that altered your thinking and subsequent focus?

H.S.: I was surprised that mitochondrial translation varies greatly among cells, even in the same cell type. I would say that the cause of the heterogeneity of mitochondrial translation found in this experiment is worth exploring in future.

What are some of the landmark moments that provoked your interest in science or your development as a scientist?

H.S.: The experience of the entire process, including manuscript preparation, revision, etc., made me grow up. Everything was fresh and a lesson for me because this is my first time engaging in a paper as a first author.

If you were able to give one piece of advice to your younger self, what would that be?

Y.K.: Only those who make up their mind quickly can seize an opportunity.

Are there specific individuals or groups who have influenced your philosophy or approach to science?

Y.K.: As a master course student, I first learned how to face and enjoy science in the Tomari Lab, The University of Tokyo. This really helped me to boost my PhD work in the Iwasaki Lab, RIKEN.

How did you decide to work together as co-first authors?

Yusuke started this work. Upon his graduation, Hironori took over the project to wrap up.